Vaccine 37 (2019) 7041–7051

Contents lists available at ScienceDirect

Vaccine

journal homepage: www.elsevier.com/locate/vaccine

Process intensification for Peste des Petites Ruminants Virus vaccine production

Marcos Sousa [a,b], Christel Fenge [c,1], Jens Rupprecht [c], Alexander Tappe [c], Gerhard Greller [c], Paula Alves [a,b], Manuel Carrondo [a], António Roldão [a,b,*]

[a] Instituto de Biologia Experimental e Tecnológica, Apartado 12, Oeiras 2780-901, Portugal
[b] Instituto de Tecnologia Química e Biológica António Xavier, Universidade Nova de Lisboa, Av. da República, 2780-157 Oeiras, Portugal
[c] Sartorius Stedim Biotech GmbH, August-Spindler-Str. 11, 37079 Göttingen, Germany

ARTICLE INFO

Article history:
Received 11 February 2019
Received in revised form 17 May 2019
Accepted 2 July 2019
Available online 8 August 2019

Keywords:
Vero cells
Microcarrier technology
In-situ cell detachment
Perfusion
Scale-up

ABSTRACT

Process intensification for Peste des Petites Ruminants Virus (PPRV) vaccine production in anchorage dependent Vero cells is challenging, involving substantial amount of bioprocess development.

In this study, we describe the implementation of a new, scalable bioprocess for PPRV vaccine production in Vero cells using serum-free medium (SFM), microcarrier technology in stirred-tank bioreactors (STB), *in-situ* cell detachment from microcarriers and perfusion. Vero cells were successfully adapted to ProVero™-1 SFM, reaching growth rates similar to serum-containing cultures (0.030 1/h *vs* 0.026 1/h, respectively). An *in-situ* cell detachment method was successfully implemented, with efficiencies above 85%. Up to 2.5-fold increase in maximum cell concentration was obtained using perfusion when compared to batch culture. Combining perfusion with the *in-situ* cell detachment method enabled the scale-up to 20 L STB directly from a 2 L STB, surpassing the need for a mid-scale platform (i.e. 5 L STB) and thus reducing seed train duration. Head-to-head comparison of cell growth and PPRV production in the 2 L and 20 L STB was performed, and no significant differences could be observed. Estimated infectious PPRV titers in Tissue Culture Infection Dose ($TCID_{50}$) ($TCID_{50}$/mL = 5×10^6 and $TCID_{50}$/cell = 5) are within the log-range reported in literature for PPRV production in STB and SFM by Silva *et al.* (2008), thus confirming the feasibility and scalability of the seed train designed [1].

The novel and scalable vaccine production process herein proposed has the potential to assist the upcoming Peste des Petites Ruminants (PPR) Global Eradication Program (targeted by FAAO for 2030) by providing African local and/or regional manufacturers with a platform capable of generating over 25,000 doses of Nigeria 75/1 strain in just 19 days using a 20 L STB.

1. Introduction

Peste des Petites Ruminants (PPR) is a highly contagious disease affecting small ruminants in Africa, Middle East and India [2]. Disease is caused by a Morbillivirus virus from the Paramyxoviridae family, antigenically related to the Rinderpest virus [2,3]. With a relevant negative economic impact of 1.45–2.1 billion USD per year [4], it is estimated that more than 60% of global domestic small ruminant population (greater than1.2 billion) is at risk of getting infected with PPRV [5]; PPR has become the next veterinary disease for eradication (targeted by FAAO for 2030), after the successful eradication of Rinderpest in 2011 [6,7].

Presently, the most effective manner to control PPR in endemic regions is vaccination [8]. PPR vaccine Nigeria strain 75/1 is the only vaccine authorized for sheep and goats immunization conferring solid protection for periods of 3 years using low viral concentration vaccine doses of approximately 10^3 $TCID_{50}$/dose [9–13]. PPRV Nigeria strain 75/1 was attenuated in Vero (African green monkey kidney) cell cultures [11] and is currently produced using the same cell line in planar, 2D culture systems (e.g. roller-bottle and cell factory) [1]. To support the upcoming PPR global eradication program, a novel vaccine production process capable of surpassing the bottlenecks of these methodologies (i.e. high cost and limited scalability) is essential. The platform implemented by Silva *et al.* (2008) provides already a step forward in that direction, with microcarrier-based stirring cultures (spinner flasks) and serum-free medium (SFM) being used for PPR vaccine production [1]. However, further developments are still needed such as the implementation of scalable production systems (e.g. STB) and reduction

* Corresponding author at: Instituto de Biologia Experimental e Tecnológica, Apartado 12, Oeiras 2780-901, Portugal.
E-mail address: aroldao@ibet.pt (A. Roldão).
[1] Present address: GE Healthcare Bio-Sciences AB, Björkgatan 30, SE-751 84 Uppsala, Sweden.

https://doi.org/10.1016/j.vaccine.2019.07.009
0264-410X/

of production time using process intensification (e.g. *in-situ* cell detachment and perfusion).

Vero cells are traditionally cultured in serum containing medium (SCM) [14–16]. However, the un-defined composition, batch-to-batch variability and contamination source of serum makes it an highly undesirable supplement in vaccine production processes [17]. Adapting a cell to SFM might be challenging, as the beneficial effect of serum on protecting cells from shear stress is lost, commonly interfering with its growth and virus production ability [18]. This becomes more evident at large-scale, with the added (negative) impact of O_2 and CO_2 gradients on cell's physiological state [19]. Despite the difficulties, Vero cells growth in SFM has been successfully demonstrated [1,20–22].

Anchorage dependent cell culture at industrial scale requires the use of microcarrier's technology. Determining the agitation requirements for microcarrier-based bioreactor cultures is key for a successful scale-up strategy. It must guarantee homogenous environment while avoiding exposing cells to shear stress levels that induce cell growth cessation, detachment or death [18]. An engineering evaluation of culture systems and operation conditions is critical for a successful implementation of this technology during scale-up of a vaccine production process [23]. In STB, scale-up is generally performed keeping constant bioengineering parameters such as energy dissipation rate (EDR), Kolmogorov eddy size (KES) and shear stress rate (SSR) [24,25]. Several authors have established threshold for those parameters [26–29]. Nonetheless, scale-up is not linear [30] and must be dealt on the case-by-case basis; keeping low shear levels while maintaining STB homogenous state, avoiding microcarriers sedimentation [18] and maintaining cell growth [24,25].

The culture of anchorage dependent cells for seed-train preparation requires cell detachment from microcarriers. This is mostly performed by enzymatic digestion using recombinant and non-animal derived proteases or trypsin-like enzymes, and requires complex steps such as PBS washing (removal of proteases inhibition proteins) and addition of proteases inhibitors [31]. Non-enzymatic procedures are less reported, but theoretically reduce cell damaged or limit changes cell's phenotype [32,33]. Cell migration by bead-to-bead cell transfer is one example [34], a technique highly dependent on cell line and nature of the microcarrier [31,35]. Recently, Nienow and co-workers (2014) described a new protocol for mesenchymal stem cell harvesting combining enzymatic and mechanical detachment [36]. The method is based on the theory that short periods of intense agitation in the presence of a suitable enzyme should enhance cell detachment from relatively large microcarriers. The results shown by the authors are promising; however, this routine has not been described for larger-scale settings than 5 L STB.

Perfusion is a commonly used operation mode to control the macro-environment of a given culture, maximizing cell growth and product formation [37]. It can be also used to achieve high-cell density cultures during seed-train preparation [38,39], surpassing mid-scale platform and thus reducing seed-train preparation time.

In this study, we developed of a new, scalable bioprocess for PPRV vaccine production in Vero cells using SFM, microcarrier technology in STB, *in-situ* cell detachment from microcarriers and perfusion. This platform is capable of generating over 25,000 doses of Nigeria 75/1 strain in just 19 days using a 20 L STB.

2. Material and methods

2.1. Cell line and culture conditions

Vero African Green monkey kidney cells (Catalog number 84113001, ECACC) routinely culture in DMEM supplemented with 10% (v/v) of FBS were adapted to grow in ProVero™-1 serum free medium (SFM) (Lonza) supplemented with 5 μg/L of Epithelial Growth Factor (EGF) and 0.1% (v/v) Pluronic® F-68. At the end of the adaptation process, a master cell bank was generated by freezing cells in CryoStor® CS-10 cryopreservation medium (Sigma) and stored in N_2 liquid (vapor phase).

2.1.1. Growth in static culture

Cells were routinely sub-cultured to 1–2 × 10^4 cell/cm^2 every 3–4 days when confluency is reached in tissue culture flasks (225 cm^2) or roller-bottles (1700 cm^2) using TrypLE Select Enzyme (1×) (Gibco) for cell detachment and Trypsin inhibitor (1 mg/mL, dissolved in cell culture medium) (Sigma) for protease inactivation. Cultures were kept at 37 °C in humidified atmosphere of 5% CO_2.

2.1.2. Growth in stirred tanks

Spinner cultures were performed in Wheaton® vessels (125 mL working volume – wv) at 37 °C and 50 rpm. Cells were seeded at a concentration of 0.1 × 10^6 cell/mL and cultured on 3 g/L of Cytodex™-1 microcarrier (prepared according to manufacturing instructions). Microcarrier colonization was promoted using continuous stirring.

Bioreactor cultures were performed in Biostat DCU-3 (2 L wv) and Biostat Cplus (20 L wv) (Sartorius). All bioreactors were equipped with two 3-blade segment impellers, 30° angled, appropriate for homogeneous mixing at low shear rates. An internal stainless steel spin-filter (cell-microcarrier retention device) of pore size 75 μm (Sartorius) was mounted on the 2 L STB only for perfusion cultures. STB process control and monitoring were carried out using Multi Fermenter Control Software (Sartorius). Dissolved oxygen was controlled at 40% (in air) by sequentially varying the percentage of N_2 and O_2 in gas inlet using a dual aeration strategy: (i) 0–2 days post-inoculation, aeration was performed via headspace at 0.1 vvm; (ii) >2 days post-inoculation, aeration was performed via submerged ring-sparger with pore diameter of 0.8 mm (0.005 vvm). Anti-foam C (Sigma) at a concentration of 0.01% (v/v) was added before starting sparging aeration. pH was controlled at 7.2 using the addition of CO_2 or $NaHCO_3$. Temperature was set to 37 °C. Stirring conditions were defined based on bioengineering correlations (see Section 2.5 and Table 1). Cells were seeded at a concentration of 0.1 × 10^6 cell/mL and cultured on 3 g/L of Cytodex™-1 microcarrier. Microcarrier colonization was promoted using intermittent stirring for 5 h: ON for 2 min at corresponding N_{FS} (Table 1) and OFF for 18 min. For perfusion cultures, cells were grown to 0.4 × 10^6 cell/mL (day 2), after which a dilution rate of 0.5–1 d^{-1} was applied to maintain glutamine and glucose above limiting concentrations, 1.5 and 5 mM, respectively.

2.2. Vero cells detachment from microcarriers

2.2.1. Enzymatic method

The enzymatic method consisted in: (i) turn off agitation and allow microcarriers to settle-down for 15 min; (ii) remove spent medium and wash microcarriers twice with PBS at 50 RPM (Spinner) or 60 RPM (2 L STB) for 10 min; (iii) remove PBS and add TrypLE Select (ratio of 1.5 volumes of TrypLE Select to 1 volume of settled microcarriers); (iv) agitate continuously the cell-microcarriers suspension for 20–25 min at 50 RPM (Spinner) or 60 RPM (2 L STB); (v) add Trypsin inhibitor (1 mg/mL, dissolved in cell culture medium) (ratio of 1 volumes of Trypsin inhibitor to 1 volume of TrypLE Select) once maximum cell detachment is reached; (vi) turn off agitation and allow microcarriers to settle-down for 20 min; (vii) harvest supernatant-containing cells and centrifuge at 200 xg for 10 min; and (viii) re-suspend cell pellet in SFM. All steps were performed at 37 °C.

Table 1
Operational conditions for microcarrier-based bioreactor cultures.

Bioreactor scale (L)			2	20
Agitation rate for off-bottom suspension of microcarriers, N_{FS} (RPM)			120	65
Agitation rate for cell culture, N_C (RPM)			70–99	33–47
Mean specific energy dissipation rate, $\bar{\varepsilon}_T$ ($\times 10^3$ W/kg or $m^2\ s^{-3}$) $\bar{\varepsilon}_T = \frac{P_0 \cdot N^3 \cdot D_i^5}{V}$	Average		0.5–1.4	0.5–1.4
Maximum local energy dissipation rate, $(\varepsilon_T)_{max}$ ($\times 10^3$ W/kg or $m^2\ s^{-3}$) $(\varepsilon_T)_{max} = P_0 \cdot N^3 \cdot D_i^2 \cdot \frac{T^2 H}{V}$ $(\varepsilon_T)_{max} = \frac{P_0 \cdot N^3 \cdot D_i^3}{(\pi/4) \cdot W_i}$	At impeller	Asm #1	8–22	5–14
		Asm #2	20–57	11–31
Kolmogorov length scale, λ (μm) $\lambda = \sqrt[4]{\frac{\nu^3}{\varepsilon}}$	Average		164–126	164–126
	At impeller	Asm #1	82–63	91–70
		Asm #2	64–50	75–58
Shear stress rate, τ (N/m^2) $\tau = \left(\frac{\varepsilon}{\nu}\right)^{\frac{1}{2}} \cdot \mu$	Average		0.02–0.03	0.02–0.03
	At impeller	Asm #1	0.07–0.12	0.06–0.10
		Asm #2	0.12–0.20	0.09–0.15
Tip speed, TS (m/s) $TS = \pi \cdot N \cdot D_i$		At Impeller	0.20–0.29	0.24–0.34
Bioreactor and impeller specifications				
Bioreactor	Type		Biostat DCU-3	Biostat Cplus
	Working volume (L)		2	20
	Diameter (m)		0.122	0.26
	Height (m)		0.18	0.38
Impeller	Type		3-blade segment, 30° angled	
	Diameter (m)		0.055	0.136
	Width (m)		0.02	0.06

D_i (m) - impeller diameter; H (m) - STB height; N (1/s) - stirring rate; P_0 (dimensionless) - power number for the impeller; T (m) - STB diameter; V (m^3) - STB working volume; V_{imp} (m^3) - volume swept out by the impeller as it rotates; W_i (m) - impeller blade width; ν (m^2/s) - kinematic viscosity; μ ($N \cdot s \cdot m^2$) - viscosity of the fluid.

2.2.2. Enzymatic-mechanical method

The enzymatic and mechanical method consisted in: (i) turn off agitation and allow microcarriers to settled-down; (ii) remove spent medium and add TrypLE Select at a ratio of 1.5 volumes of TrypLE Select to 1 volume of settled microcarriers; (iii) agitate continuously the cell-microcarriers suspension for 4 cycles of 7 min at 155 rpm, with a 5 s pulse at 250 rpm in between cycles; (iv) add Trypsin inhibitor (1 mg/mL, dissolved in cell culture medium) once maximum cell detachment is reached, at a ratio of 1 volume of Trypsin inhibitor to 1 volume of TrypLE Select. All steps were performed at 37 °C.

2.2.3. Detachment efficiency

The detachment efficiency of Vero cells from microcarriers, D_{eff} (%), was defined as:

$$D_{eff} = N_{vc,AD}/N_{vc,BD} \times 100\% \quad (1)$$

where $N_{vc,AD}$ is the number of viable cells in suspension obtained after the detachment protocol and $N_{vc,BD}$ is the number of viable cells expected in the culture prior to detachment from microcarriers as estimated by crystal violet staining and trypan blue dye exclusion methods (see Section 2.6.1 for details).

2.3. Bead-to-bead transfer of Vero cells

Vero cells were cultured on 3 g/L of Cytodex™-1 microcarrier in a 2 L STB until confluence is reached. Confluent microcarriers were then seeded to a new 2 L STB containing bare microcarriers at a ratio of 4:1 (bare:confluent) and bead-to-bead cell transfer promoted by intermittent mode of agitation, i.e. 2 min ON at 80–100 RPM and 28 min OFF, for 48 h. All steps were performed at 37 °C.

2.3.1. Bead-to-bead transfer efficiency

The bead-to-bead transfer efficiency of Vero cells, BtB_{eff} (%), was defined as:

$$BtB_{eff} = N_{cMC}/N_{bMC} \times 100\% \quad (2)$$

where N_{cMC} is the number of colonized microcarriers and N_{bMC} is the total number of microcarriers in the culture after the bead-to-bead transfer protocol.

2.4. Production of PPRV

Vero cells at 0.2×10^6 cell/mL were infected with PPRV Nigeria 75/1 virus strain, kindly provided by Dr. Geneviève Libeau (CIRAD-EMVT, France), at a multiplicity of infection (MOI) of 0.01 $TCID_{50}$/-cell. Prior to infection, one complete medium exchange was performed. Cultures were harvested at day 5–6 post-infection. For bioreactor cultures, microcarriers were allowed to settle-down and PPRV bulk clarified using depth filters with 75 μm pore size and 0.018 m^2 (Sartopure PP3, 2 L STB) or 0.12 m^2 (Sartopure PP3, 20 L STB) area.

2.5. Bioengineering correlations

Operational conditions including stirring rates and scale-up criteria were estimated using the bioengineering correlations Kolmogorov eddy size, shear stress rate and tip speed, as described elsewhere [28,27,36]. The power input, P (W or $kg \cdot m^2/s^3$), throughout the STB can be determined by:

$$P = P_0 \cdot \rho \cdot N^3 \cdot D_i^5 \quad (3)$$

where P_0 is the power number for the impeller (1.2 for both 2L and 20L STB, [40]), ρ is medium density (kg/m^3), N (1/s) is the stirring

rate, and D_i (m) the impeller diameter. The specific power input, P/M, or mean specific energy dissipation rate, $\bar{\varepsilon}_T$ (W/kg or m^2/s^3), can be estimated by:

$$\frac{P}{M} = \bar{\varepsilon}_T = \frac{P_0 \cdot N^3 \cdot D_i^5}{V} \quad (4)$$

were M (kg) is the fluid mass and V (m^3) is the STB working volume. Notwithstanding the substantial data already known on the flow and turbulence levels in STB, the estimation of maximum local energy dissipation rate, $(\varepsilon_T)_{max}$, still remains challenging with multiple approximate relations that can be used for such. In this study, two different assumptions (Asm) were considered for estimating $(\varepsilon_T)_{max}$ [41–43]:

$$\text{Asm } \#1 \quad (\varepsilon_T)_{max}/\bar{\varepsilon}_T \ \frac{T^2 H}{D_i^3}, \quad \text{from [41]} \quad (5)$$

$$\text{Asm } \#2 \quad (\varepsilon_T)_{max} = (\varepsilon_T)_{imp} = \frac{P}{\rho V_{imp}}, \quad \text{from [42,43]} \quad (6)$$

where T (m) is the STB diameter, H (m) the STB height, and V_{imp} (m^3) is the volume swept out by the impeller as it rotates. V_{imp} is defined by $(\pi/4)\ D_i^2\ W_i$ [55], in which W_i (m) is the impeller blade width. Based on these, $(\varepsilon_T)_{max}$ was estimated by:

$$(\varepsilon_T)_{max} = P_0.N^3.D_i^2.\frac{T^2 H}{V}, \quad \text{from [41]} \quad (7)$$

$$(\varepsilon_T)_{max} = \frac{P_0.N^3.D_i^3}{(\pi/4).W_i}, \quad \text{from [42,43]} \quad (8)$$

The Kolmogorov eddy size (KES), λ (μm), and the shear stress rate (SSR), τ (N/m^2) can be estimated by:

$$\lambda = (\nu/\varepsilon)^{1/4} \quad (9)$$

$$\tau = (\varepsilon/\nu)^{1/2} \cdot \mu \quad (10)$$

where ν (m^2/s) is the kinematic viscosity, and μ ($N{\cdot}s{\cdot}m^2$) is the viscosity of the fluid. The viscosity of the fluid (0.0071 g/cm·sec) and the kinematic viscosity (0.007 cm^2/sec) used for calculations were taken from literature for a microcarrier-based cell culture performed at 37 °C [28]. The tip speed, TS (m/s) can be estimated by:

$$TS = \pi \cdot N \cdot D_i \quad (11)$$

The agitation rate needed for off-bottom suspension of microcarriers, i.e. fully re-suspend settled-down microcarriers, N_{FS} (1/s), can be calculated using the Zwietering equation as proposed by Ibrahim & Nienow [44]:

$$N_{Fs} = S \cdot \nu^{0.1} \cdot d_p^{0.2} \cdot (g \cdot \Delta\rho/\rho)^{0.45} X^{0.13}/D_i^{0.85} \quad (12)$$

where S (6.4, [45]) is a dimensionless parameter, d_p (147–248 μm for Cytodex™-1, with average diameter of approximately 190 μm according to manufacturer) is the diameter of microcarriers, g (9.8 m/s^2) is the gravity acceleration, Δρ (kg/m^3) is the density difference between submerged microcarriers and fluid, and X (%, w/w) is the weight ratio between microcarriers and fluid.

2.6. Analytics

2.6.1. Cell counting and viability

Total cell concentration was estimated using crystal violet staining. Briefly, after cells disruption with solution of 0.1 M citric acid with 1% (v/v) Triton X-100 incubated for at least 1 h at 37 °C with agitation, nuclei were stained with 0.1% (w/v) crystal violet and counted in a hemocytometer chamber. Viable cell concentration was estimated using Fuchs–Rosenthal hemocytometer chamber and trypan blue dye exclusion method. Microcarrier colonization was assessed by staining cells with fluorescein diacetate (FDA, green, viable cells) and propidium iodide (PI, red, dead cells) followed by visual inspection under a fluorescence microscope as described in Serra *et al.* [46].

2.6.2. Metabolite analysis

Glutamine, glucose and lactate concentrations were determined using YSI 7100MBS (YSI Incorporated). Ammonia concentration was quantified enzymatically using a commercially available UV test (Nzytech). All samples were analyzed in triplicate. The specific consumption or production rates, q_X (pmol/cell·h) were estimated applying a general mass balance equation for a batch or perfusion system as described elsewhere [47].

2.6.3. PPRV titration

Virus titer was determined using $TCID_{50}$ protocol as described by Silva *et al.* [1]. Briefly, 100 μL of viral samples 10-fold serial diluted in MEM supplemented with 10% (v/v) of FBS and 100 μL of Vero cells suspension (2×10^4/well) were prepared and transfer to 96-well microtiter plate. Plates were kept at 37 °C in humidified atmosphere of 5% CO_2 and cytopathic effect checked microscopically at day 10. Data collected was analyzed using GraphPad Prism software (4-parameters variable slope) estimating virus titers in $TCID_{50}$.

3. Results

3.1. Vero cells adaptation to ProVero™-1 serum-free medium

Vero cells adaptation to ProVero™-1 SFM was performed using a step-wise strategy. It consisted in sub-culturing cells in tissue culture flasks using SFM supplemented with progressively reduced percentages of FBS, namely 5%, 2.5%, 1.25% and 0%. Prior to each FBS reduction stage, at least 3 cell passages were needed to achieve constant specific growth rate (μ). Results are shown in Fig. 1. Control culture (DMEM supplemented with 5% FBS) and adapted culture (ProVero™-1 SFM) have similar growth rates, μ = 0.026 ± 0.006 1/h *vs* μ = 0.030 ± 0.006 1/h, respectively. Likewise, maximum cell concentrations achieved in control ($1.9 \pm 0.5 \times 10^5$ cell/cm^2) and adapted ($1.8 \pm 1.0 \times 10^5$ cell/cm^2)

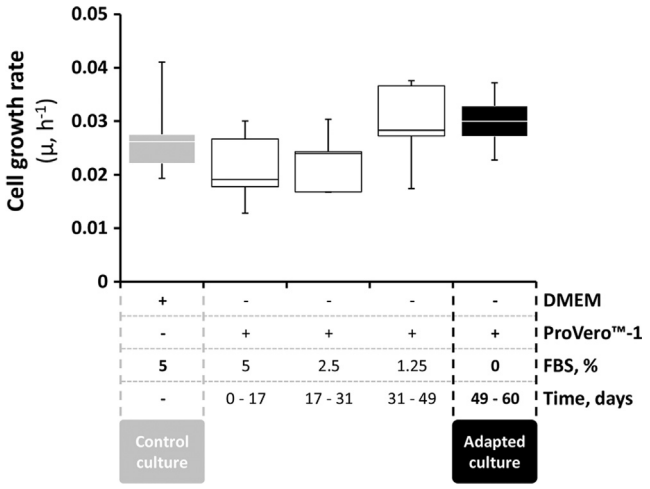

Fig. 1. Whiskers chart of Vero cells growth rate (μ) during the adaptation process to serum free conditions. Control culture: cells growing in DMEM supplemented with 5% (v/v) of FBS. Adapted culture: cells growing in ProVero™-1 SFM. Horizontal lines are medians, boxes represent the interquartile range and error bars show the full range of estimated rates.

cultures were remarkably similar. These results confirm that Vero cells adaptation to SFM was successfully achieved.

3.2. Determining agitation requirements for microcarrier-based bioreactor cultures

The minimum agitation rate for cell culture, $N_{c,min}$, was defined as the stirring needed to ensure that microcarriers are uniformly suspended and oxygen mass transfer is sufficient to support cell growth and product formation. The $N_{c,min}$ used for the 2 L STB has been selected based on work previously done in-house [48,49]. To define the $N_{c,min}$ of the 20 L STB, hydrodynamic parameters were computed, including: the EDR, KLS, SSR and TS (Eqs. (3)–(11)). By retaining constant the power input *per* volume (P/V) as the scale-up criteria from 2 L to 20 L, it was possible to estimate the $N_{c,min}$ of the 20 L STB (33 RPM) (Table 1).

The maximum agitation rate for cell culture, $N_{c,max}$, was defined as the stirring needed to start inducing cell growth inhibition and/or cell death. The study of Croughan and co-workers on the correlation between KLS and cell growth was herein used to assist the definition of $N_{c,max}$ for the 2 L and 20 L STB [28]. The theory is that KLS lower than 2/3 of microcarrier's diameter have significant, immediate impact on cell growth [28]. Assuming that average diameter of Cytodex™-1 microcarrier is 190 μm, the stirring rate inducing a KES of 126 μm in the 2 L STB is 99 RPM, and thus this was the rate considered as $N_{c,max}$ (Table 1). By retaining constant the P/V as the scale-up criteria from 2 L to 20 L, it was possible to estimate the $N_{c,max}$ of the 20 L STB (47 RPM) (Table 1).

Overall, the operational conditions ($N_{c,min}$ and $N_{c,max}$) defined for the 2 L and 20 L STB were within non-detrimental SSR (<0.2 N/m^2, [26,27]) and tip speed (<0.4 m/s, [26,27]) values (Table 1).

The agitation rate needed for off-bottom suspension of microcarriers, i.e. fully re-suspend settled-down microcarriers, N_{FS}, was calculated using Eq. (12) [44]. The values obtained for the 2 L and 20 L STB were 155 and 73, respectively. *In situ* testing revealed that these agitation rates were 12–29% higher than those experimentally assessed by visual inspection/monitoring. Therefore, to minimize the impact of stirring on cell growth, the N_{FS} observed experimentally for the 2 L (120 RPM) and 20 L (65 RPM) STB were the ones used throughout the experiments (Table 1).

3.3. Improved seed-train process for inoculation of a 20 L bioreactor

Conventional seed-train process for inoculation of a 20 L STB begins with thawing of a cryopreserved working cell bank vial, followed by successive expansions into larger culture vessels: (i) 225 cm^2 T-flask, (ii) 1700 cm^2 roller bottle, (iii) 2 L STB, and (iv) 5 L STB. This approach presents two mains challenges: (i) the strategy for scale-up of Vero cells in microcarrier-based bioreactor cultures, and (ii) the number of N-1 seed train bioreactors needed.

3.3.1. Detachment-reattachment as strategy for scale-up of Vero cells in microcarrier-based bioreactor cultures

Two strategies for scale-up of Vero cells in microcarrier cultures were evaluated: I. bead-to-bead transfer, and II. detachment-reattachment (Fig. 2). Experiments were performed in 2 L STB. In

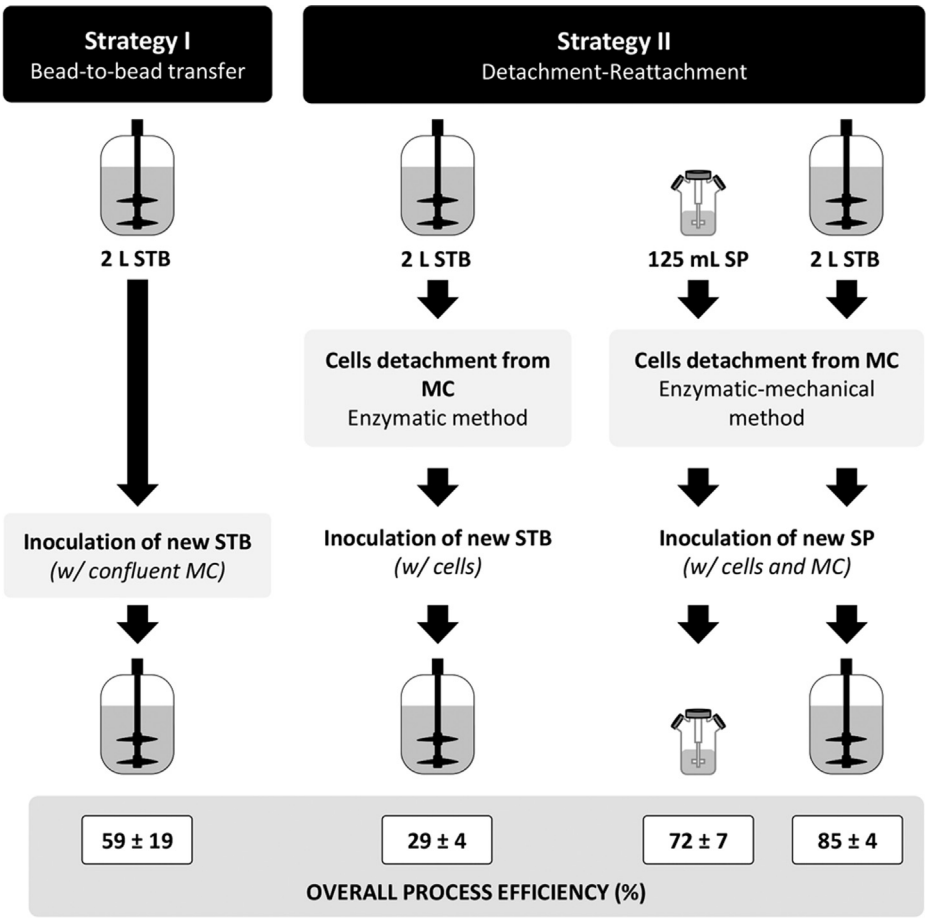

Fig. 2. Strategies for scale-up of Vero cells in microcarrier-based bioreactor cultures. Overall process efficiency (%) using bead-to-bead transfer (Strategy I) and detachment-reattachment (Strategy II). Data are mean ± standard deviation obtained from at least three independent biological replicates (n = 3). STB: stirred tank bioreactor; SP: spinner flask; MC: microcarrier.

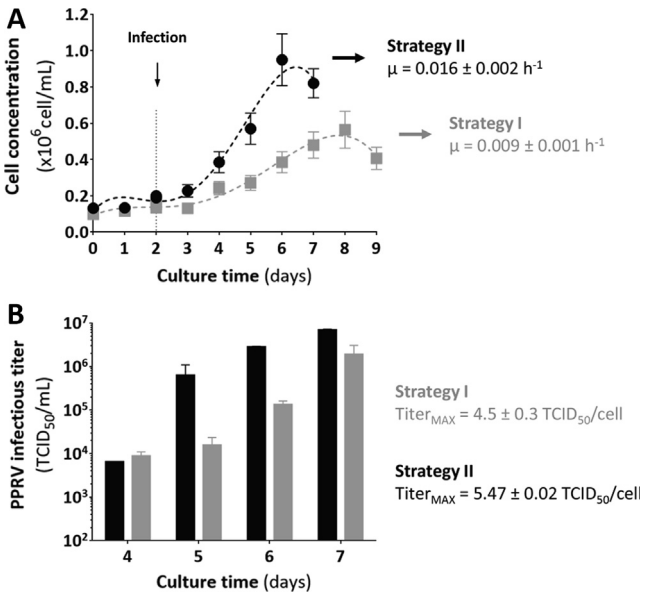

Fig. 3. Impact of the strategy for scale-up of Vero cells in microcarrier-based bioreactor cultures on growth kinetics (A) and PPRV production (B). Strategy I: bead-to-bead transfer; Strategy II: detachment-reattachment using the enzymatic method. Experiments were performed in 2 L STB. Data are mean ± standard deviation obtained from at least three independent measurements (n = 3).

Strategy I, bead-to-bead cell transfer was promoted as described in M&M (see Section 2.3), with overall process efficiency (BtB_{eff}, Eq. (2)) of 59 ± 18%, meaning that over 41% of microcarriers remained empty until the end of the production run. In **Strategy II**, cells were detached from microcarriers using the enzymatic method as described in M&M (see Section 2.2.1), with detachment efficiency (D_{eff}, Eq. (1)) of 35 ± 7%. Two reasons for this low value were: (i) inefficient detachment process as cells remained attached to microcarriers even after 20–25 min in TrypLE Select, and (ii) cell loss during PBS washing and harvesting procedures. The reattachment process was more efficient (95 ± 4%), giving an overall process efficiency of 29 ± 4%. Cells obtained from both strategies were then used for PPRV production (Fig. 3). The kinetics of cell growth and virus production are considerably different, with cells from **Strategy I** presenting lower specific growth rate, peak viable cell concentration and maximum PPRV titers than those achieved with cells from **Strategy II**. These results suggest that detachment-reattachment as cell culture seed-train strategy is better than bead-to-bead transfer. However, the overall process efficiency is low (≈30%) and thus require optimization.

3.3.2. Improving detachment efficiency using an enzymatic-mechanical method

To better understand the basics of Vero cells detachment from microcarriers, and therefore optimize D_{eff}, a set of experiments were designed and run in 125 mL spinner flasks (Fig. 4). Results obtained show that: (i) increasing the concentration of TrypLE Select does not improve D_{eff} and has a negative impact on cell viability; (ii) combining short period of intense agitation with the presence of TrypLE Select increases D_{eff} without impacting on cell viability; and (iii) removing the PBS washing step prior to cell detachment has no impact on D_{eff} (Fig. 4A). Based on this data, an enzymatic-mechanical method for Vero cells detachment from microcarriers was proposed (see **M&M**, Section 2.2.2). Head-to-head comparison of cells obtained from the two methods (enzymatic *vs* enzymatic-mechanical) was performed in 125 mL spinner flasks, with no significant differences in the kinetics of cells reattachment to microcarriers, cell growth and PPRV production being observed (Fig. 4B). The *in-situ* cells detachment method was successfully scaled-up to 2 L STB, with D_{eff} of 85 ± 4% (Fig. 2).

3.3.3. Perfusion strategy to reduce the number of N-1 seed train bioreactors needed

To achieve higher cell densities in the N-1 seed train bioreactor, and thus reduce the time to production bioreactor, a perfusion strategy was explored. First, we evaluated the impact of perfusion on Vero cells growth in 2 L STB (Fig. 5A). Growth rate and cell confluence on microcarriers was higher in perfusion than in batch. In addition, cell concentration of up to 2.4×10^6 cell/mL could be achieved using perfusion, contrasting with the 1×10^6 cell/mL obtained in batch. The metabolic profile of cells were assessed, and specific rates estimated (Table 2). No significant differences in major nutrients (glucose and glutamine) consumption or by-product (lactate) formation were observed between both culture systems, and values recorded were within the normally obtained for animal cell cultures [50]. The exception is the specific NH_3 production rate, which was 2-fold higher in perfusion than in batch. The follow-up study consisted in assessing the effect of cell concentration on detachment efficiency (D_{eff}) (Fig. 5B). Experiments were performed in 2 L STB operated in perfusion and using the enzymatic-mechanical method as cell detachment strategy. Results show that D_{eff} is dependent on the cell concentration at time of harvest, with the highest D_{eff} (≈88%) being achieved at cell concentration of 1.7×10^6 cell/mL. Lastly, the impact of perfusion on PPRV production was assessed by comparing the performance of two 2 L STB, one seeded with cells originated from batch mode and another seeded with cells originated from perfusion mode. Results are shown in Fig. 5C and demonstrate that perfusion had no impact on cell growth and PPRV production as similar kinetics (i.e. regression coefficient (b) and Pearson's correlation (r) close to 1) were obtained in both conditions tested.

Based on aforementioned data, the perfusion strategy for the N-1 seed train bioreactor will be implemented when scaling-up PPRV vaccine production from 2 L to 20 L STB.

3.4. Scale-up PPRV vaccine production from 2 L to 20 L STB

The feasibility and scalability of the seed-train strategy herein proposed (i.e. perfusion for the N-1 bioreactor followed by detachment-reattachment using the enzymatic-mechanical cell detachment method) was demonstrated by comparing performances of the 2 L and 20 L STB for cell growth and PPRV production (Fig. 6).

The kinetics of microcarrier colonization for the two STB are presented in Fig. 6A. More than 90% of microcarriers were colonized within the first 24 h post inoculation, with no significant differences being observed between both culture systems. Likewise, cell growth and PPRV production in the 2L and 20L STB followed similar kinetics (Fig. 6B). Cells were able to grow until day 4 post-infection, reaching maximum concentrations of $0.9–1 \times 10^6$ -cell/mL, after which cell concentration and viability started decreasing. This growth kinetics is typical of cell cultures infected at low MOIs (<1 virus/cell) and/or with viruses having impaired replication capacity (e.g. attenuated PPRV Nigeria 75/1 virus strain herein used), and has been previously observed elsewhere [1,11]. The morphology of Vero cells during PPRV infection process is shown in Fig. 6C. In both STB, cells are attached and spread on microcarriers at the time of infection (day 0 PI), become swollen as infection progresses (day 3 PI), and start lysing and/or detaching from microcarriers at day 5 PI. Metabolic profiles of cells before and after infection were assessed, and specific rates estimated (Table 2). No significant differences were observed between both systems, and recorded values are within those normally obtained

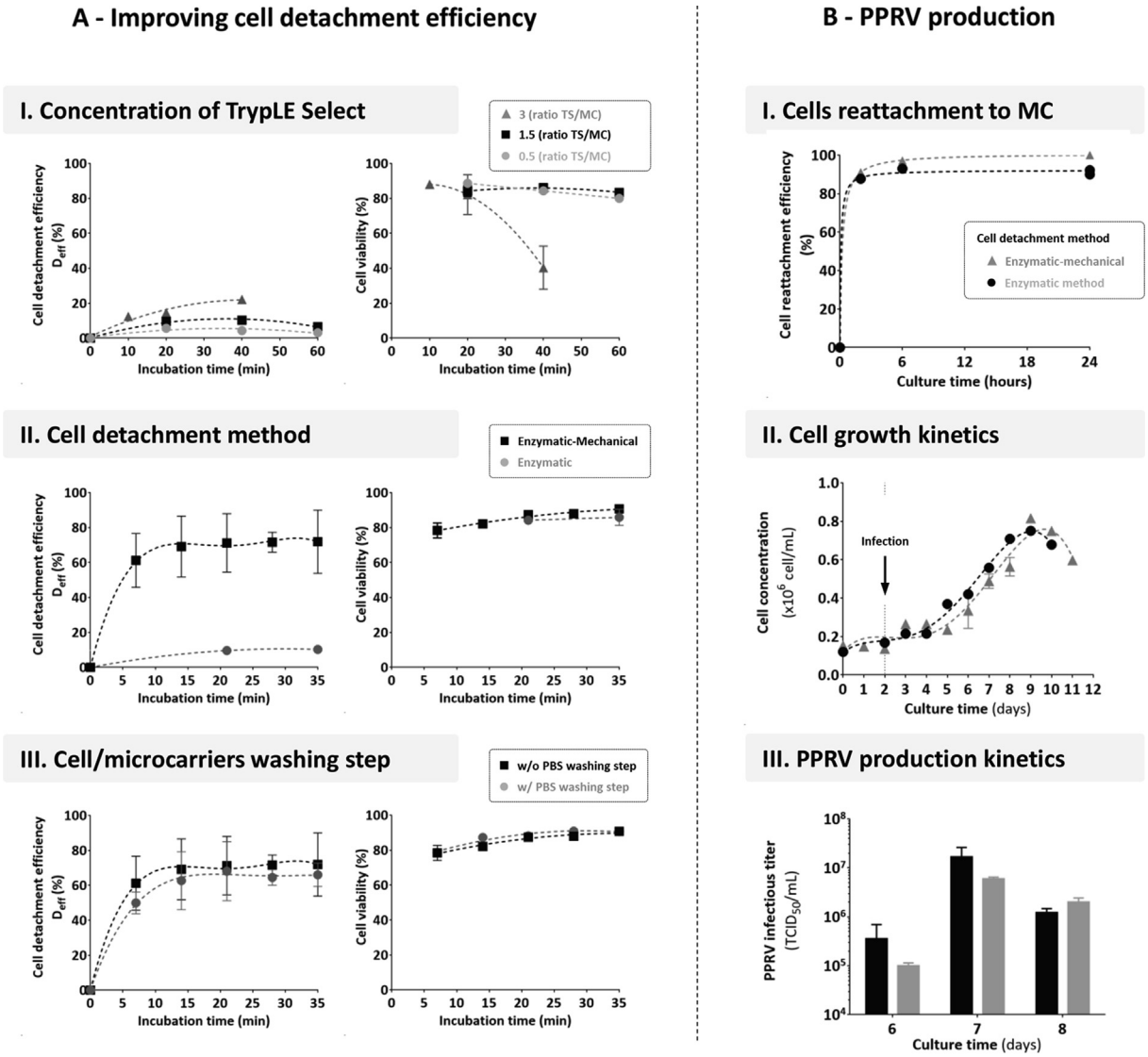

Fig. 4. Implementation of an enzymatic-mechanical method for Vero cells detachment from microcarriers. Panel A - Improving cell detachment efficiency by evaluating the impact of: (I) cell-dissociation enzyme, (II) cell detachment method, and (III) cell/microcarriers PBS washing step, on cell detachment efficiency (D_{eff}, %) and cell viability. Panel B - Head-to-head comparison of two cell detachment methods for: (I) cell reattachment efficiency, (II) cell growth kinetics, and (III) PPRV production kinetics. Experiments were performed in Wheaton® spinner vessels (125 mL working volume). Data are mean ± standard deviation obtained from at least three independent measurements (n = 3).

for batch cultures [50]. Infectious PPRV titers of approx. 5×10^6 - $TCID_{50}$/mL or 5 $TCID_{50}$/cell were achieved at day 4–5 post-infection irrespective of the culture system. These titers are within those reported in literature for PPRV production in STB and SFM [1]. Finally, PPRV recovery yields after clarification by depth filtration were comparable (85 ± 9% in the 2L STB and 90 ± 17% in the 20L STB).

4. Discussion

Process intensification for PPRV vaccine production in anchorage dependent Vero cells is challenging, involving substantial amount of bioprocess development. In this study we developed a new, scalable bioprocess for PPRV vaccine production based on Vero cells and microcarrier technology in bioreactors, using ProVero™-1 as serum-free medium (SFM), an enzymatic-mechanical method for *in-situ* cell detachment from microcarriers, and perfusion. This process will ultimately support the eradication program of PPR targeted by the Food and Agriculture Organization (FAAO) for 2030 [6–8].

One of the aims of this work was to adapt Vero cells to SFM. SFM is preferable not only from an economic perspective (process costs are potentially reduced) but also from a safety standpoint (eliminates the risk of unwanted contamination originated from the use of bovine serum) [51]. Using a stepwise adaptation strategy we were able to minimize the impact of switching from serum-containing to serum-free medium on cell's physiological state, with growth rates varying from 0.022 1/h to 0.029 1/h throughout the adaptation process (Fig. 1). Cell's ability to attach and detach from microcarriers was not compromised, and aggregation was not observed. Importantly, cell growth rate in SFM is similar to control culture and literature data [1,21,22,52].

Determining the agitation requirements for microcarrier-based bioreactor cultures is key for a successful scale-up strategy. Cells growing on microcarriers are sensible to increases on energy dissipation and shear forces, associated to the agitation and aeration rates applied for homogenous mixing (microcarriers are uniformly

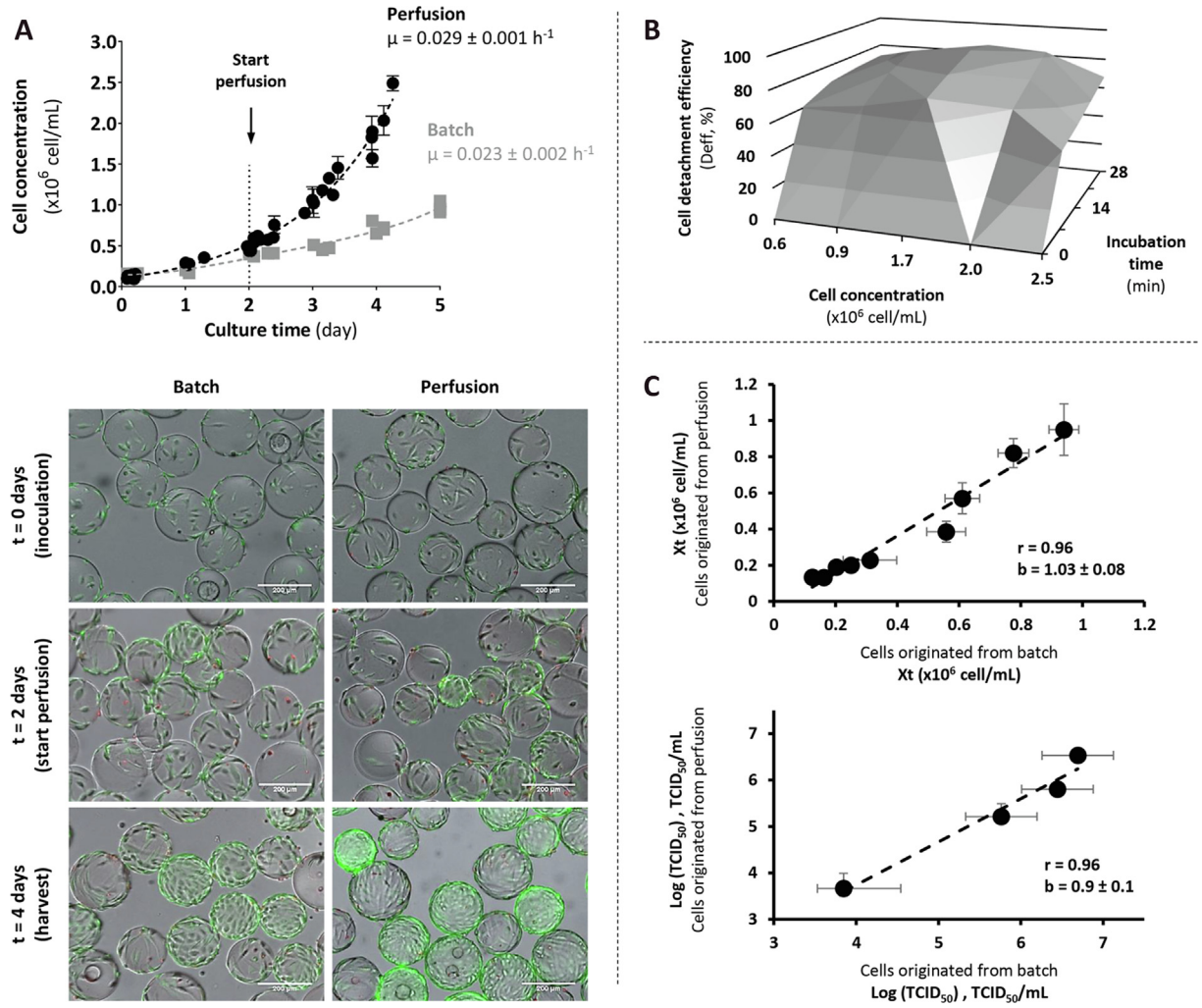

Fig. 5. Impact of perfusion on Vero cells growth and PPRV production. (A) Cell growth kinetics in batch (grey symbols) and perfusion (black symbols); experiments were performed in 2 L STB. Immunofluorescence microscopy images of cells growing in batch and perfusion are shown (green: live cells stained with fluorescein diacetate; red: dead cells stained with propidium iodide; scale bars: 200 μm). (B) Correlation of cell detachment efficiency (D_{eff}, %) with cell concentration and incubation time with cell-dissociation enzyme; experiments were performed in 125 mL Spinner flasks. (C) linear regression of total cell concentration (X_T, cell/mL) (upper panel) and PPRV infectious titer ($TCID_{50}$/mL) (lower panel) from cells originated from batch and perfusion, with ensuing Pearson's correlation (r) and regression coefficient (b); experiments were performed in 2 L STB. Data are mean ± standard deviation obtained from at least three independent biological replicates (n = 3).

Table 2
Specific rates of nutrient consumption and by-product formation during (i) Vero cells growth in batch and perfusion, and (ii) PPRV production in 2 L and 20 L STB.

Process Phase	Operation mode/Scale	Specific rates (pmol/cell·h)			
		Glucose Rate ± SD	**Glutamine** Rate ± SD	**Lactate** Rate ± SD	**Ammonia** Rate ± SD
Vero cells growth	Batch	−0.30 ± 0.03	−0.042 ± 0.004	0.55 ± 0.06	0.025 ± 0.005
	Perfusion	−0.32 ± 0.02	−0.051 ± 0.003	0.48 ± 0.04	0.053 ± 0.003
PPRV production	2 L STB	−0.31 ± 0.07	−0.04 ± 0.01	0.5 ± 0.1	0.024 ± 0.006
	20 L STB	−0.22 ± 0.01	−0.058 ± 0.005	0.30 ± 0.03	0.05 ± 0.02

Cultures were performed as described in Materials and Methods. Three independent biological replicates (n = 3) were considered for assessing specific rates during Vero cells growth; a single production run (n = 1) was considered for assessing specific rates during PPRV production. Negative values indicate nutrient consumption. SD - standard deviation (SD).

suspended) and efficient oxygen transfer [23]. Aiming at providing bioengineering correlations to guide bioprocess engineers during process development, Croughan *et al.* (1987) have established a relationship between KLS and cell growth identifying a critical KES threshold above which no harm to cells occurs [28]. In microcarrier-based cultures this corresponds to 2/3 of microcarrier's diameter, which for our culture system using Cytodex™-1 would be 126 μm. Recently, Nienow *et al.* (2016) reported that KLS as small as 30% of microcarrier diameter can be used for human mesenchymal stem cell cultures without negatively impacting on cell proliferation and quality attributes [53]. Based on these results, one could speculate that Vero cells may withstand higher shear levels than those reported in earlier studies. However, since this has not been experimentally validated, the KES threshold

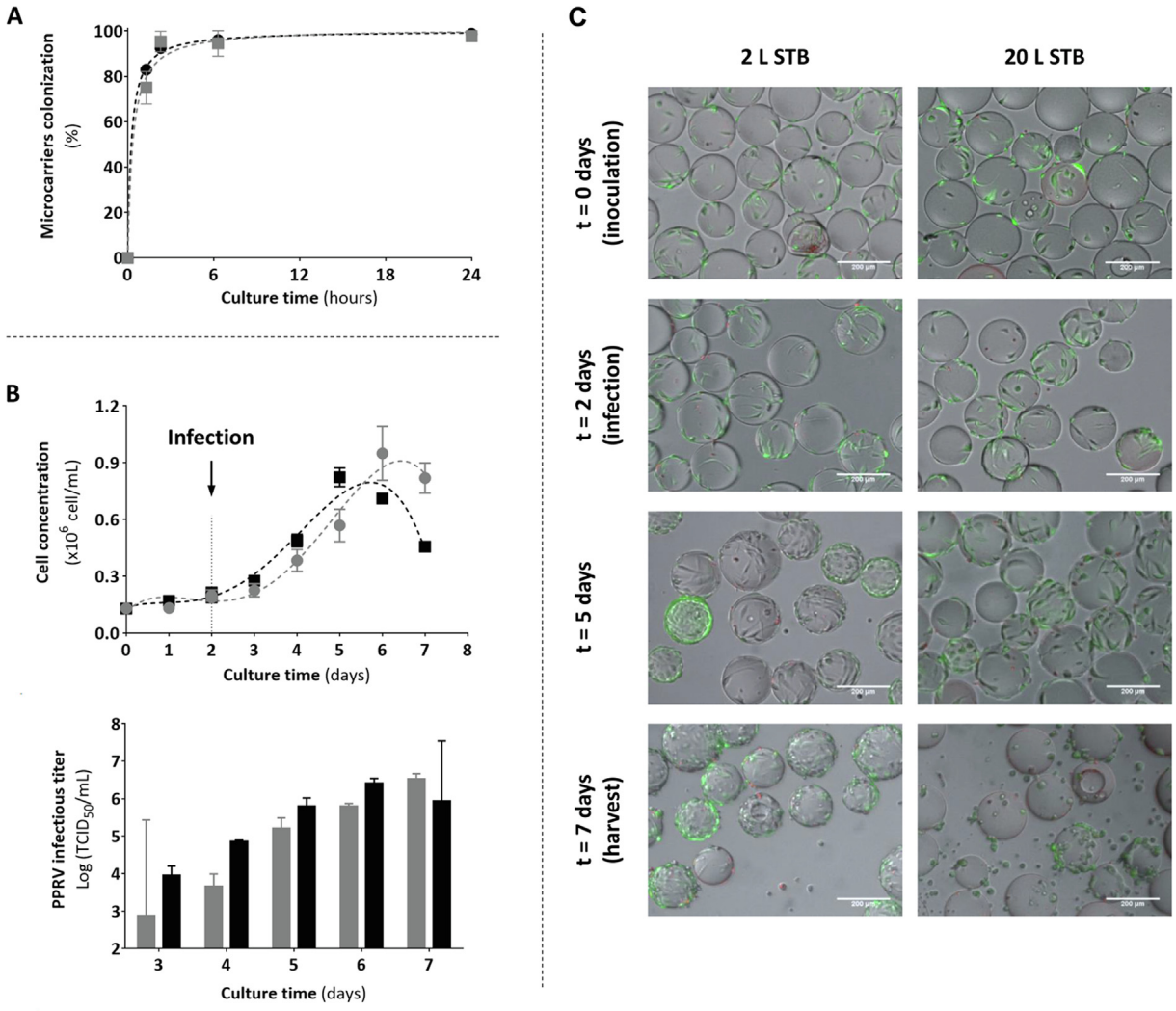

Fig. 6. Scale-up PPRV vaccine production from 2 L to 20 L STB. Kinetics of (A) microcarriers colonization, (B) cell growth and PPRV production for the 2 L STB (grey symbols and bars) and 20 L STB (black symbols and bars) using a MOI of 0.01 $TCID_{50}$/cell. (C) Immunofluorescence microscopy images of cells growing in the two culture systems (green: live cells stained with fluorescein diacetate; red: dead cells stained with propidium iodide; scale bars: 200 μm). Data expressed as mean ± standard deviation (relative to three measurements of microcarriers colonization, cell concentration and PPRV titer).

of 2/3 of microcarrier's diameter as described by Croughan *et al.* (1987) was kept as our main criteria for setting the agitation requirements [28]. In two other studies, Nienow (1998) and Cherry and Papoutsakis (1989) proposed that cell damage is proportional to the increase in average energy dissipation rate and microcarriers size [54,27]. In fact, it is stated that SSR below 0.7 N/m^2 and TS below 0.4 m/s have reduced impact on cell growth. To comply with these limits, the maximum agitation rates for the 2 L and 20 L STB were set to 99 RPM and 47 RPM, respectively (Table 1). At such operational conditions, KES, SSR and TS are below their respective thresholds, thus ensuring optimal process conditions for cell growth.

Another parameter to account for in microcarrier-based cultures is the agitation rate needed for off-bottom suspension of microcarriers (N_{FS}). Settled-down microcarriers must be fully re-suspended at a minimized power input per unit of volume to limit the impact of agitation on cell growth. This is particularly important during seed train process, as often multiple N-1 bioreactors are needed and microcarrier colonization is promoted via intermittent stirring. N_{FS} can be estimated using the Zwietering equation [44]. However, in over 50% of carefully executed microcarrier studies (incl. our study), its value is overestimated [44]. George *et al.* (2010) observed identical discrepancies but using a different bioreactor design [55]. Nienow *et al.* (2016) strongly suggest to visual assess the N_{FS} value and, then, estimate S value for that impeller type [53]. These findings suggest that N_{FS} determination must be done experimentally, as done in this study (Table 1).

The ability of Vero cells in microcarrier-based cultures to detach and reattach or to migrate to new/bare microcarriers is limited, posing a major problem for process seed train and scale-up [31]. Therefore, revising the basis of cell detachment and reattachment to microcarriers is important, in particular when cells are cultivated in SFM and non-animal origin reagents. Recently, a new protocol for mesenchymal stem cell harvesting from microcarriers has been proposed, which is based on the theory that short periods of intense agitation in the presence of a suitable enzyme should enhance cell detachment from relatively large microcarriers [36]. Once in suspension, cells should not be damaged since their diameter is smaller than KES. Based on this theory, we developed an enzymatic-mechanical method for *in-situ* Vero cells detachment from Cytodex™-1 microcarriers. Upon fine-tuning (i.e. elimination of PBS washing prior to cell detachment and centrifugation for

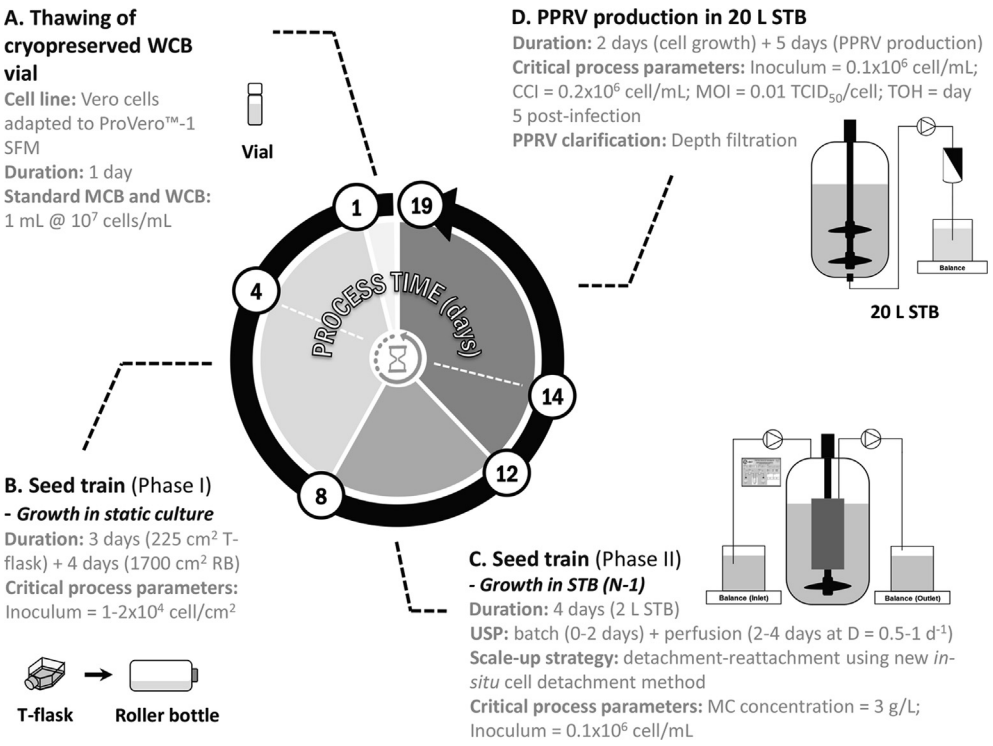

Fig. 7. New, scalable bioprocess for PPRV vaccine production in Vero cells using serum-free medium and microcarrier technology in bioreactors. CCI: cell concentration at infection; D: dilution rate; MCB: master cell bank; MOI: multiplicity of infection; RB: roller bottle; TOH: time of harvest; WCB: working cell bank.

removal of protease-inhibitor mix), this method provided a significant improvement in overall process efficacy (≈85%) when compared to detachment-reattachment strategy using enzymatic method (≈29%) or bead-to-bead transfer (≈59%) (Fig. 2). This value is in-line with what is reported in literature for Vero cells growing in a SFM [22].

The number of N-1 seed train bioreactors is critical for the economic viability of any vaccine production platform. Keeping this number to its minimum reduces process time and production cost. Therefore, strategies capable of maximizing cell concentration before detachment must be consider and evaluated accordingly. In this study, perfusion was explored as strategy to achieve higher cell densities in the N-1 seed train bioreactor. Up to 2-fold increase in growth rate and cell concentration was obtained when compared to batch processes, with peak cell density being achieved one day earlier (Fig. 5). The perfusion strategy combined with the *in-situ* cell detachment enabled scale-up to 20L directly from 2L, surpassing a mid-scale platform (i.e. 5 L STB) and thus reducing seed train duration.

Head-to-head comparison of cell growth and PPRV production in the 2 L and 20 L STB was performed (Fig. 6). No significant differences were observed between both culture systems, with infectious PPRV titers of $5x10^6$ $TCID_{50}$/mL being achieved 4–5 days post-infection. Silva *et al.* (2008) reported similar values for PPRV production in STB and SFM, i.e. maximum infectious PPRV titers around 10^6 $TCID_{50}$/mL and 5–8 $TCID_{50}$/cell achieved between day 4 and 6 post-infection [1]. Together, the results aforementioned confirm the feasibility and scalability of the new bioprocess for PPRV vaccine production in Vero cells herein proposed (Fig. 7).

5. Conclusion

This work demonstrates the suitability of a new, scalable bioprocess for PPRV vaccine production in Vero cells using serum-free medium and microcarrier technology in bioreactors (Fig. 7). Over 25,000 doses of Nigeria 75/1 strain can be potentially generated in just 19 days using a 20 L STB. Due to its small footprint and fast turn-around time, this process may allow African local and/or regional manufacturers to produce high quantities of PPRV vaccine in short time-frames, supporting the eradication program of PPR targeted by FAAO for 2030.

Acknowledgements

This work was supported by Sartorius Stedim Biotech and received financial support from Fundação para a Ciência e Tecnologia through the Investigador FCT programme 2014 (project IF/01704/2014 and IF/01704/2014/CP1229/CT0001) and from iNOVA4 Health Research Unit (LISBOA-01-0145-FEDER-007344), which is cofunded by Fundação para a Ciência e Tecnologia/Ministério da Ciência e do Ensino Superior, through national funds, and by FEDER under the PT2020 Partnership Agreement. The authors wish to thank Carina Silva, Margarida Serra and João Clemente for technical and scientific support. The authors are also grateful to Dr. Geneviève Libeau (CIRAD-EMVT, France) for providing the PPR vaccine strain. The authors express their gratitude to Dr. Carlos Augusto for the fruitful discussions during the setup of this work. *Conflict of interest:* all authors declare no conflict of interest and agree with the submission of the manuscript, which was not submitted for publication elsewhere.

References

[1] Silva AC, Delgado I, Sousa MFQ, Carrondo MJT, Alves PM. Scalable culture systems using different cell lines for the production of Peste des Petits ruminants vaccine. Vaccine 2008;26:3305–11. https://doi.org/10.1016/j.vaccine.2008.03.077.

[2] Parida S, Muniraju M, Mahapatra M, Muthuchelvan D, Buczkowski H, Banyard AC. Peste des petits ruminants. Vet Microbiol 2015;181:90–106. https://doi.org/10.1016/j.vetmic.2015.08.009.

[3] Gibbs DPJ, Taylormichael WP, Lawman JP, Bryant J. Classification of Peste des petits ruminants virus as the fourth member of the genus morbillivirus. Intervirology 1979;11:268–74. https://doi.org/10.1159/000149044.

[4] de Haan NC, Kimani T, Rushton J, Lubroth J. Why is small ruminant health important—Peste des petits ruminants and its impact on poverty and

Economics? In: Munir M, editor. BT - Peste des Petits Ruminants Virus. Berlin, Heidelberg: Springer Berlin Heidelberg; 2015. p. 195–226. https://doi.org/10.1007/978-3-662-45165-6_12.
[5] Peste Des FAO. Petitis Ruminants (PPR): a challenge for small ruminants' production. Animal Production and Health Division; 2009.
[6] Dhinakar Raj G, Thangavelu A, Munir M. Strategies and Future of Global Eradication of Peste des Petits Ruminants Virus BT - Peste des Petits Ruminants Virus. In: Munir M, editor., Berlin, Heidelberg: Springer Berlin Heidelberg; 2015, p. 227–54. https://doi.org/10.1007/978-3-662-45165-6_13..
[7] Mariner JC, Jones BA, Rich KM, Thevasagayam S, Anderson J, Jeggo M, et al. The opportunity to eradicate Peste des petits ruminants. J Immunol 2016;196:3499–506. https://doi.org/10.4049/jimmunol.1502625.
[8] Bora M, Yousuf RW, Dhar P, Singh RP. An overview of process intensification and thermo stabilization for upscaling of Peste des petits ruminants vaccines in view of global control and eradication. VirusDisease 2018;29:285–96. https://doi.org/10.1007/s13337-018-0455-3.
[9] Singh R, Vinayagamurthy B, Veerakyathappa B, Sen A, Saravanan P, Yadav M. Possible control and eradication of Peste des petits ruminants from India: Technical aspects. Vet Ital 2009;45:449–62.
[10] Taylor WP, Abegunde A. The isolation of peste des petits ruminant virus from Nigerian sheep and goats. Res Vet Sci 1979;26:94–6.
[11] Diallo A, Taylor WP, Lefevre PC, Provost A. Attenuation of a strain of rinderpest virus: potential homologous live vaccine. Rev Elev Med Vet Pays Trop 1989;42:311–9.
[12] Diallo A, Minet C, Le Goff C, Berhe G, Albina E, Libeau G, et al. The threat of peste des petits ruminants: progress in vaccine development for disease control. Vaccine 2007;25:5591–7. https://doi.org/10.1016/j.vaccine.2007.02.013.
[13] Diallo A. Peste des Petits ruminants. Manual of diagnostic tests and vaccines for terrestrial animals, vols. I and II; 2004.
[14] Montagnon BJ, Fanget B, Vincent-Falquet JC. Industrial-scale production of inactivated poliovirus vaccine prepared by culture of Vero cells on microcarrier. Clin Infect Dis 1984;6:S341–4. https://doi.org/10.1093/clinids/6.Supplement_2.S341.
[15] Barrett PN, Mundt W, Kistner O, Howard MK. Vero cell platform in vaccine production: moving towards cell culture-based viral vaccines. Exp Rev Vacc 2009;8:607–18. https://doi.org/10.1586/erv.09.19.
[16] Gallo-Ramírez LE, Nikolay A, Genzel Y, Reichl U. Bioreactor concepts for cell culture-based viral vaccine production. Exp Rev Vacc 2015;14:1181–95. https://doi.org/10.1586/14760584.2015.1067144.
[17] Falkner E, Appl H, Eder C, Losert UM, Schöffl H, Pfaller W. Serum free cell culture: the free access online database. Toxicol Vitr 2006;20:395–400. https://doi.org/10.1016/j.tiv.2005.09.006.
[18] Merten O-W. Advances in cell culture: anchorage dependence. Philos Trans R Soc B Biol Sci 2015;370:20140040. https://doi.org/10.1098/rstb.2014.0040.
[19] Clapp KP, Castan A, Lindskog EK. Upstream processing equipment. Biopharm Process Dev Des Implem Manuf Process 2018:457–76. https://doi.org/10.1016/B978-0-08-100623-8.00024-4.
[20] Butler M, Burgener A, Patrick M, Berry M, Moffatt D, Huzel N, et al. Application of a serum-free medium for the growth of Vero cells and the production of reovirus. Biotechnol Prog 2000;16:854–8. https://doi.org/10.1021/bp000110+.
[21] Petiot E, El-Wajgali A, Esteban G, Gény C, Pinton H, Marc A. Real-time monitoring of adherent Vero cell density and apoptosis in bioreactor processes. Cytotechnology 2012;64:429–41. https://doi.org/10.1007/s10616-011-9421-2.
[22] Rourou S, van der Ark A, van der Velden T, Kallel H. A microcarrier cell culture process for propagating rabies virus in Vero cells grown in a stirred bioreactor under fully animal component free conditions. Vaccine 2007;25:3879–89. https://doi.org/10.1016/j.vaccine.2007.01.086.
[23] Sousa MFQ, Silva MM, Giroux D, Hashimura Y, Wesselschmidt R, Lee B, et al. Production of oncolytic adenovirus and human mesenchymal stem cells in a single-use, Vertical-Wheel bioreactor system: impact of bioreactor design on performance of microcarrier-based cell culture processes. Biotechnol Prog 2015;31:1600–12. https://doi.org/10.1002/btpr.2158.
[24] Cruz PE, Cunha A, Peixoto CC, Clemente J, Moreira JL, Carrondo MJT. Optimization of the production of virus-like particles in insect cells. Biotechnol Bioeng 1998;60:408–18. https://doi.org/10.1002/(SICI)1097-0290(19981120)60:4<408::AID-BIT2>3.0.CO;2-Q.
[25] Maranga L, Cunha A, Clemente J, Cruz P, Carrondo MJT. Scale-up of virus-like particles production: effects of sparging, agitation and bioreactor scale on cell growth, infection kinetics and productivity. J Biotechnol 2004;107:55–64. https://doi.org/10.1016/j.jbiotec.2003.09.012.
[26] Cherry RS, Papoutsakis ET. Growth and death rates of bovine embryonic kidney cells in turbulent microcarrier bioreactors. Bioprocess Eng 1989;4:81–9. https://doi.org/10.1007/BF00373735.
[27] Cherry RS, Papoutsakis ET. Physical mechanisms of cell damage in microcarrier cell culture bioreactors. Biotechnol Bioeng 1988;32:1001–14. https://doi.org/10.1002/bit.260320808.
[28] Croughan MS, Hamel JF, Wang DI. Hydrodynamic effects on animal cells grown in microcarrier cultures. Biotechnol Bioeng 1987;29:130–41. https://doi.org/10.1002/bit.260290117.
[29] Croughan MS, Hamel JP, Wang DIC. Effects of microcarrier concentration in animal cell culture. Biotechnol Bioeng 1988;32:975–82. https://doi.org/10.1002/bit.260320805.
[30] Varley J, Birch J. Reactor design for large scale suspension animal cell culture. Cytotechnology 1999;29:177. https://doi.org/10.1023/A:1008008021481.
[31] Merten O-W. Cell detachment. Encycl Cell Technol. American Cancer Society; 2003. p. 1–12. , https://doi.org/10.1002/0471250570.spi036.
[32] Rappaport C. Review-progress in concept and practice of growing anchorage-dependent mammalian cells in three dimension. Vitr Cell Dev Biol - Anim 2003;39:187–92.
[33] Li B, Wang X, Wang Y, Gou W, Yuan X, Peng J, et al. Past, present, and future of microcarrier-based tissue engineering. J Orthop Transl 2015;3:51–7. https://doi.org/10.1016/j.jot.2015.02.003.
[34] Wang Y, Ouyang F. Bead-to-bead-transfer of vero cells in microcarrier culture. Bioprocess Eng 1999;31:221–4. https://doi.org/10.1007/s004490050665.
[35] Rafiq Q, Ruck S, Hanga M, Heathman T, Coopman K, Nienow A, et al. Qualitative and quantitative demonstration of bead-to-bead transfer with bone marrow-derived human mesenchymal stem cells on microcarriers: utilising the phenomenon to improve culture performance. Biochem Eng J 2018;135:11–21. https://doi.org/10.1016/j.bej.2017.11.005.
[36] Nienow AW, Rafiq QA, Coopman K, Hewitt CJ. A potentially scalable method for the harvesting of hMSCs from microcarriers. Biochem Eng J 2014;85:79–88. https://doi.org/10.1016/j.bej.2014.02.005.
[37] Bielser JM, Wolf M, Souquet J, Broly H, Morbidelli M. Perfusion mammalian cell culture for recombinant protein manufacturing – A critical review. Biotechnol Adv 2018;36:1328–40. https://doi.org/10.1016/j.biotechadv.2018.04.011.
[38] Castilho LR, Medronho RA. Cell Retention Devices for Suspended-Cell Perfusion Cultures BT - Tools and Applications of Biochemical Engineering Science. In: Schügerl K, Zeng A-P, Aunins JG, Bader A, Bell W, Biebl H, et al., editors., Berlin, Heidelberg: Springer, Berlin Heidelberg; 2002, p. 129-69. https://doi.org/10.1007/3-540-45736-4_7.
[39] Clincke MF, Mölleryd C, Zhang Y, Lindskog E, Walsh K, Chotteau V. Very high density of CHO cells in perfusion by ATF or TFF in WAVE bioreactor™: Part I: effect of the cell density on the process. Biotechnol Prog 2013;29:754–67. https://doi.org/10.1002/btpr.1704.
[40] Kaiser S, Löffelholz C, Werner S, Eibl D. CFD for characterizing standard and single-use stirred cell culture bioreactors. Comput Fluid Dyn Technol Appl 2011:97–122. https://doi.org/10.5772/23496.
[41] Placek J, Tavlarides LL. Turbulent flow in stirred tanks. Part I: turbulent flow in the turbine impeller region. AIChE J 1985;31:1113–20. https://doi.org/10.1002/aic.690310709.
[42] McManamey WJ. Sauter mean and maximum drop diameters of liquid-liquid dispersions in turbulent agitated vessels at low dispersed phase hold-up. Chem Eng Sci 1979;34:432–4. https://doi.org/10.1016/0009-2509(79)85081-2.
[43] Pacek AW, Chamsart S, Nienow AW, Bakker A. The influence of impeller type on mean drop size and drop size distribution in an agitated vessel. Chem Eng Sci 1999;54:4211–22. https://doi.org/10.1016/S0009-2509(99)00156-6.
[44] Ibrahim S, Nienow AW. Suspension of microcarriers for cell culture with axial flow impellers. Chem Eng Res Des 2004;82:1082–8. https://doi.org/10.1205/cerd.82.9.1082.44161.
[45] Atiemo-Obeng VA, Penney WR, Kresta SM. Solid-liquid mixing. In: Paul E, Atiemo-Obeng VA, Kresta SM, editors. John Wiley Sons, Wiley-Interscience. John Wiley & Sons, Inc.; 2004. p. 543–84. https://doi.org/10.1002/0471451452.ch10.
[46] Serra M, Brito C, Sousa MFQ, Jensen J, Tostões R, Clemente J, et al. Improving expansion of pluripotent human embryonic stem cells in perfused bioreactors through oxygen control. J Biotechnol 2010;148:208–15. https://doi.org/10.1016/j.jbiotec.2010.06.015.
[47] Abecasis B, Aguiar T, Arnault Émilie, Costa R, Gomes-Alves P, Aspegren A, et al. Expansion of 3D human induced pluripotent stem cell aggregates in bioreactors: bioprocess intensification and scaling-up approaches. J Biotechnol 2017;246:81–93. https://doi.org/10.1016/j.jbiotec.2017.01.004.
[48] Marcelino I, Sousa MFQ, Veríssimo C, Cunha AE, Carrondo MJT, Alves PM. Process development for the mass production of *Ehrlichia ruminantium*. Vaccine 2006;24:1716–25. https://doi.org/10.1016/j.vaccine.2005.08.109.
[49] Fernandes P, Peixoto C, Santiago VM, Kremer EJ, Coroadinha AS, Alves PM. Bioprocess development for canine adenovirus type 2 vectors. Gene Ther 2012;20:353–60.
[50] Zeng AP, Hu WS, Deckwer WD. Variation of stoichiometric ratios and their correlation for monitoring and control of animal cell cultures. Biotechnol Prog 1998;14:434–41. https://doi.org/10.1021/bp9800337.
[51] Giangaspero M. Pestivirus species potential adventitious contaminants of biological products. Trop Med Surg 2013;1:1–6.
[52] Quesney S, Marc A, Gerdil C, Gimenez C, Marvel J, Richard Y, et al. Kinetics and metabolic specificities of Vero cells in bioreactor cultures with serum-free medium. Cytotechnology 2003;42:1–11. https://doi.org/10.1023/A:1026185615650.
[53] Nienow AW, Hewitt CJ, Heathman TRJ, Glyn VAM, Fonte GN, Hanga MP, et al. Agitation conditions for the culture and detachment of hMSCs from microcarriers in multiple bioreactor platforms. Biochem Eng J 2016;108:24–9. https://doi.org/10.1016/J.BEJ.2015.08.003.
[54] Nienow AW. Hydrodynamics of stirred bioreactors. Appl Mech Rev 1998;51:3–32. https://doi.org/10.1115/1.3098990.
[55] George M, Farooq M, Dang T, Cortes B, Liu J, Maranga L. Production of cell culture (MDCK) derived Live Attenuated Influenza Vaccine (LAIV) in a fully disposable platform process. Biotechnol Bioeng 2010;106:906–17. https://doi.org/10.1002/bit.22753.